Original Article

Abnormal spindle-like microcephaly-associated protein promotes proliferation by regulating cell cycle in epithelial ovarian cancer

Yiguo Wu[1#], Yujuan You[2#], Ling Chen[1], Yue Liu[3], Yujuan Liu[4], Weiming Lou[5], Fen Fu[1]

[1]Department of Obstetrics and Gynecology, The Second Affiliated Hospital of Nanchang University, Nanchang, China; [2]Department of Anesthesiology, The Second Affiliated Hospital of Nanchang University, Nanchang, China; [3]Queen Mary School, Medical College of Nanchang University, Nanchang, China; [4]Department of Obstetrics and Gynecology, The Third Affiliated Hospital of Nanchang University, Nanchang, China; [5]Institute of Translational Medicine, Nanchang University, Nanchang, China

Contributions: (I) Conception and design: Y Wu, Y You, F Fu; (II) Administrative support: Y Liu, F Fu; (III) Provision of study materials or patients: Y Wu, Y You, Y Liu; (IV) Collection and assembly of data: L Chen, Y Liu, Y Liu, W Lou; (V) Data analysis and interpretation: Y Wu, Y You, L Chen; (VI) Manuscript writing: All authors; (VII) Final approval of manuscript: All authors.

[#]These authors contributed equally to this work.

Correspondence to: Fen Fu. The Second Affiliated Hospital of Nanchang University, No.1 Mingde Road, Nanchang 330000, China. Email:fu_fen@163.com.

Background: Epithelial ovarian cancer (EOC) ranks first for female gynecological tumor-related deaths. Due to the limited efficacy of traditional chemotherapy strategies, potential therapeutic targets are urgently needed. Previous studies have reported a relationship between abnormal spindle-like microcephaly-associated protein (ASPM) and ovarian cancer based on immunohistochemistry (IHC) and bioinformatics analysis. However, the potential role of ASPM in the proliferation of ovarian cancer cells and its molecular mechanism remain to be elucidated. Therefore, we aimed to further investigate the potential role of ASPM and its underlying mechanism in EOC using integrated online databases, clinical samples, and cell models.

Methods: We used online databases (Gene Expression Profiling Interactive Analysis, Cbioportal and Kaplan-Meier Plotter) to analyze differential ASPM expression in ovarian carcinoma and explore its prognostic value in ovarian cancer (OvCa) patients. Immunohistochemistry staining based on a clinical tissue microarray (TMA) comprised 75 cases of EOC tissue and 5 cases of adjacent normal ovary tissue was used to detect the ASPM expression and analyze the relationship between ASPM expression and EOC characteristics. Various cell function experiments related to tumorigenesis were performed including the CCK8 assay, 5-ethynyl-2'-deoxyuridine (EdU), colony formation assay and Transwell assay in EOC cell models (A2780 and OVCAR3) with knocked down ASPM by small interfering RNA (siRNA) to observe its role. Finally, Kyoto Encyclopedia of Genes and Genomes (KEGG) pathway enrichment was conducted to determine the signaling pathways in which ASPM was involved in the pathogenesis of ovarian cancer. Analysis of cell cycle distribution using flow cytometry was further performed to verify the pathways.

Results: The expression profile based on data from The Cancer Genome Atlas (TCGA) database confirmed ASPM expression in EOC was higher compared with normal tissue, and further analysis suggested that higher expression was correlated with worse patient prognosis. Immunohistochemical analysis further indicated that ASPM was highly expressed in OvCa tissues and associated with a higher pathological stage, grade, and positive lymphatic metastasis. Cell models with knocked down ASPM by small interfering RNA (siRNA) significantly inhibited proliferation and migration. KEGG pathway enrichment and cell cycle analysis showed that ASPM silencing could inhibit ovarian cancer cell proliferation via synthesis (S) phase arrest.

Conclusions: Our study confirmed that ASPM promoted proliferation and caused S phase arrest in EOC cells. ASPM may become a potential molecular marker for early screening and a valuable therapeutic target in EOC.

© Gland Surgery. All rights reserved.

Keywords: Abnormal spindle-like microcephaly-associated protein (ASPM); epithelial ovarian cancer (EOC); prognosis; proliferation

Submitted Dec 22, 2021. Accepted for publication Mar 20, 2022.
doi: 10.21037/gs-22-29
View this article at: https://dx.doi.org/10.21037/gs-22-29

Introduction

Ovarian cancer (OvCa), ranked fifth for tumor-related mortality in women, is the most lethal malignant tumor of the reproductive system in the United States (1), seriously affecting women's health and quality of life. More than 80% of OvCa originates from epithelial tissue [epithelial ovarian cancer (EOC)], which includes the following 4 subtypes: serous adenocarcinoma, clear cell carcinoma, endometrioid adenocarcinoma, and mucinous adenocarcinoma (2). Because early clinical symptoms are rarely detected and lack specificity, most patients are diagnosed at a late clinical stage, which is often too late to achieve favorable outcomes from surgery and first-line chemotherapy (3). Despite the advanced therapeutic efficacy of some chemotherapy drugs, the overall 5-year survival rate of OvCa patients remains low at approximately 30–40% (4). Therefore, the discovery of effective biomarkers for early diagnosis and useful targets for improved prognosis is of considerable importance.

Abnormal spindle-like microcephaly-associated protein (ASPM) is the human homolog of the *Drosophila* mitotic spindle protein. The protein coding region is located on chromosome 1q3l and spans 62,567 base pairs (bp), with a10,906 bp open reading frame (5). ASPM is a spindle pole/intermediate protein that regulates the direction of mitosis and cytoplasmic division (6). During brain development, ASPM mainly maintains symmetric division and proliferation of neuro-epithelial cells (5). The gene MCPH5, which encodes ASPM, is related to autosomal primary microcephaly, a developmental brain disease characterized by small brain structure, which is not systematically accompanied by intellectual deficiency (7). Given that ASPM plays a crucial role in regulating the normal mitotic process of cells, its relationship with tumors has also attracted the attention of scholars. Recent studies have found that ASPM is abnormally expressed in various cancers and could predict prognosis in several types, including glioblastoma (8), endometrial adenocarcinoma (9), pancreatic carcinoma (10), and prostate adenocarcinoma (11). Based on integrated bioinformatics analysis, 2 studies identified ASPM as a potential biomarker and drug target for EOC (12,13). Brüning-Richardson *et al.* found ASPM was highly expressed in primary ovarian cultures, and the higher the grade, the higher its expression (14). However, interestingly, subsequent immunohistochemical analysis suggested cytoplasmic ASPM expression was negatively correlated with tumor grade and stage in the serous subtype of EOC (15). In addition, there is a lack of validation of cellular models of ASPM involvement in ovarian cancer progression and analysis of its mechanisms in current studies so far. Therefore, the full integration of multidimensional data, including cell function experiments, is necessary to clarify the oncogenic role of ASPM in EOC and its underlying molecular mechanisms.

Herein we describe our investigation of the role of ASPM in EOC using bioinformatics analysis, clinical tissue sample analysis, and cell phenotype experiments. We demonstrated that ASPM played an oncogenic role in EOC progression by regulating the cell cycle. Our study provides a deeper understanding of ASPM in EOC progression and may provide direction for potential therapeutic targets in the future. We present the following article in accordance with the MDAR reporting checklist (available at https://gs.amegroups.com/article/view/10.21037/gs-22-29/rc).

Methods

Bioinformatic analysis

Gene Expression Profiling Interactive Analysis (16) (GEPIA, http://gepia.cancer-pku.cn/) and cBioPortal for Cancer Genomics (17) (https://www.cbioportal.org/) were used together with data from The Cancer Genome Atlas (TCGA) to investigate differential ASPM expression in OvCa tissue and normal tissue. TCGA contains a considerable amount of RNA sequencing data, thereby providing opportunities for developing a deeper understanding of the function of genes. GEPIA and cBioPortal provide visualization tools for investigating genomic data for multiple cancers obtained from TCGA and are widely used for bioinformatics in medicine (18-20). Differential expression analysis was

© Gland Surgery. All rights reserved.

conducted by means of one-way ANOVA based on TCGA and Genotype-Tissue Expression (GTEx) data via GEPIA. Genes with log2 fold change (log2FC) cutoff >1 and P<0.05 were considered statistically significant. To further investigate ASPM gene alterations in OvCa, we used cBioPortal to analyze putative copy number alterations based on the TCGA dataset.

To evaluate the prognostic effect of ASPM, Kaplan-Meier Plotter (17,19-21) (http://kmplot.com/analysis/), an online website for assessing the prognostic value of genes in 21 types of tumors including OvCa, was used to evaluate prognostic value of ASPM. The data sources included the Gene Expression Omnibus (GEO), TCGA, and European Genome-phenome Archive (EGA) databases, which are also widely applied to bioinformatic medicine (22-24). Survival analysis was performed based on 2 groups divided by median expression.

Tissue microarray (TMA) and immunohistochemistry

TMA we purchased was acquired from Xi'an Taibos Biotechnology Co., Ltd (China) and comprised 75 cases of EOC tissue and 5 cases of adjacent normal ovary tissue confirmed by surgical pathology. All experiments were approved by the Ethics Committee of the Second Affiliated Hospital of Nanchang University [REVIEW(2020) No.(010)] and patient consent was acquired. The study was conducted in accordance with the Declaration of Helsinki (as revised in 2013).

Detection of ASPM protein expression in the TMA was determined by immunohistochemistry (IHC). In brief, clinical samples embedded in paraffin and split into 3-mm sections were heated at 72 ℃ for 2 h, followed by deparaffinization and ethanol gradient rehydration. The sections were then incubated in 3% hydrogen peroxide (H_2O_2) for 10 min to eliminate endogenous peroxidase. The sections were treated with citrate buffer2 times and then washed with phosphate-buffered saline (PBS) for antigen retrieval, followed by diluted serum incubation at 37 ℃ for 30 min to block nonspecific sites. Anti-ASPM rabbit polyclonal antibody was applied to incubate the slides at 4 ℃ overnight. The slides were washed with PBS and incubated with corresponding biotin-labelled secondary antigens and rinsed again, followed by streptavidin labelled with horseradish peroxidase (HRP). Finally, we used 3,3'-diaminobenzidine (DAB)-H_2O_2 as the chromogenic reagent for visualization, and hematoxylin was added for counterstaining.

Two pathologists were recruited to independently perform staining evaluation of the TMA according to a semiquantitative scoring system (25) based on the degree of tumor cell staining [0 (negative), 1 (weak), 2 (moderate), and 3 (strong)] and the fraction of staining [0 (0%), 1 (1–24%), 2 (25–49%), 3 (50–74%), and 4 (75–100%)]. The total IHC score of ASPM, ranging from 0 to 12, was multiplied by these 2 scores.

Cell culture and transfection

OVCAR3 cells (1101HUM-PUMC000362) and ES-2 cells (1101HUM-PUMC000371) were purchased from Cell Resource Center (Institute of Basic Medicine, Chinese Academy of Medical Sciences, Beijing, China). A2780 cells (iCell-h004) were obtained from iCell Bioscience Inc. (Shanghai, China). OVCAR3 and A2780 cells were cultured in Roswell Park Memorial Institute (RPMI) 1640 medium (Solarbio, Beijing, China) containing 20% and 10% fetal bovine serum (FBS) (Gibco, GrandIsland, NY, USA), respectively. ES-2 cells were grown in Dulbecco's modified Eagle's medium (DMEM) (Solarbio) containing 10% FBS. The 3 cell lines were maintained at 37 ℃ with 5% CO_2.

Negative control (NC) small interfering RNA (siRNA) and 2 ASPM gene-specific siRNAs were synthesized by Gene Pharma (Shanghai, China). The ASPM siRNA-NC, siRNA-1, and siRNA-2 targeted sequences were 5'-UUCUCCGAACGUGUCACG-3', 5'-GCUACUUUCAUCCAGUCUATT-3', and 5'-GCAGCAUGCCGUUUGUUUATT-3', respectively. Once the cells grew to a density of approximately 40% in a 6-well plate, they were transfected with siRNA using TurboFect Transfection Reagent (Thermo Fisher Scientific, Waltham, MA, USA).

Quantitative reverse transcription polymerase chain reaction (RT-qPCR)

Total RNA was extracted from cells using TRIzol reagent. PrimeScript RT Reagent Kit with gDNA Eraser (#RR047A, Takara, Minato-ku, Tokyo, Japan) was prepared to reverse transcribe RNA into complementary DNA (cDNA). RT-qPCR was performed using TB GreenTM Premix Ex TaqTM II (#DRR820A, Takara, Minato-ku, Tokyo, Japan) with a 7900HT Fast Real-time System (Applied Biosystems, Foster City, CA, USA). The relative messenger RNA (mRNA) level of genes was determined using the $2^{-\Delta\Delta Ct}$ method after standardization with internal control gene glyceraldehydes-3-phosphate dehydrogenase

© Gland Surgery. All rights reserved.

(GAPDH). The primers used were: (I) ASPM: forward, 5'-GGCCCTAGACAACCCTAACGA-3' and reverse, 5'-AGCTTGGTGTTTCAGAACATCA-3'; and (II) GAPDH: forward, 5'-CCACCCATGGCAAATTCCATGGCA-3' and reverse, 5'-TCTAGACGGCAGGTCAGGTCCAC-3'.

Western blot analysis

Protein was harvested using radioimmunoprecipitation (RIPA) lysis buffer (Cell Signaling Technology, Danvers, MA, USA) on ice after washing 3 times with PBS, and its concentrations were quantified using bicinchoninic acid (BCA) protein assay kits (Thermo Fisher Scientific). Sodium dodecyl sulphate-polyacrylamidegel electrophoresis (SDS-PAGE, 8%) was used for protein separation, and the protein was then transferred to a polyvinylidene difluoride (PVDF) membrane with 300 mA constant current for 2 h. After blocking with 5% nonfat milk for 1 h, the membrane was incubated with anti-rabbit-ASPM (1:1,000, #26223-1-AP, Proteintech, Chicago, IL, USA) or anti-mouse-GAPDH (1:1,000, #MAB374, Millipore, Billerica, MA, USA) at 4 ℃ overnight and then incubated with HRP-conjugated secondary antibodies under normal indoor conditions for 2 h. Finally, enhanced chemiluminescence (ECL) reagent was used to detect the protein.

Cell counting kit-8 (CCK-8) assay

CCK-8 assays were applied for detection of cell viability using CCK-8 reagents (#CA1210, Solarbio). Cells were seeded in 96-well plates in 100 μL medium at approximately 3,000 cells per well. Then, 10 μL CCK8 reagent was added to each well and incubated for 4 h with cutoff times of 12, 24, 48, 72, and 96 h. Finally, the absorbance at 450 nm was quantified using a microplate reader.

Colony formation assay

Cells were seeded at a density of 50 cells/cm^2 in a 6-well culture plate and were cultured for another 2 weeks until visible colonies were formed. Colonies were photographed and counted after fixation with formaldehyde and stain with 2% crystal violet.

5-ethynyl-2'-deoxyuridine (EdU) staining assay

Cells (5×10^3) were planted in 24-well plates after transfection. After 48 h, the cell culture medium was replaced with 50 μM diluted EdU solution and incubated for 2 h. Cells were fixed using PBS containing 4% polyformaldehyde. Cells were treated, successively, with cell-light EdU Apollo 488 and Hoechst 33342 in Vitro Kit (#C10310-3, RIBOBIO, Guangzhou, China) according to the operating instructions. Images were captured by a fluorescence microscope.

Cell migration assay

OVCAR3cells (2×10^4) and A2780 cells (1×10^5) were seeded into the 24-well Transwell chamber with serum-free RPMI 1640 medium, while the corresponding normal medium was added into the lower chamber. Cells that had penetrated the Transwell membrane were fixed with 4% paraformaldehyde and stained with 2% crystal violet after cultivation for 24 h. The migratory cells were photographed by microscopy and counted.

Potential pathway analysis

To investigate the potential pathways regulated by ASPM, we downloaded the ovarian cancer expression matrix from TCGA database at University of California Santa Cruz (UCSC) Xena (https://xenabrowser.net/) and divided patients into a high expression group or low expression group according to the median of ASPM expression. We performed differential expression analysis of the 2 groups using the "limma" package (https://bioconductor.org/packages/limma/) in R (adjusted $P<0.05$). Differentially expressed genes (DEGs) underwent Kyoto Encyclopedia of Genes and Genomes (KEGG) pathway analysis using the web-based Gene Set Analysis Toolkit (http://www.webgestalt.org/) to determine the potential pathways regulated by ASPM.

Analysis of cell cycle distribution by flow cytometry

Cells transfected with siRNA were harvested and then fixed with ice-cold 70% ethanol at –20 ℃ overnight. After centrifugation for 3 min, the cells were resuspended in 500 μL PBS. We added 100 μg/mL ribonuclease (RNase) A and 50 μg/mL propidium iodide and then incubated the cells for 30 min. Evaluation of cell status was performed using the Accuri C6 Plus flow cytometer (BD Biosciences, SanJose, CA, USA), and distribution of the cell cycle was quantified by Modfit (Verity Software House, Topsham, ME, USA).

© Gland Surgery. All rights reserved.

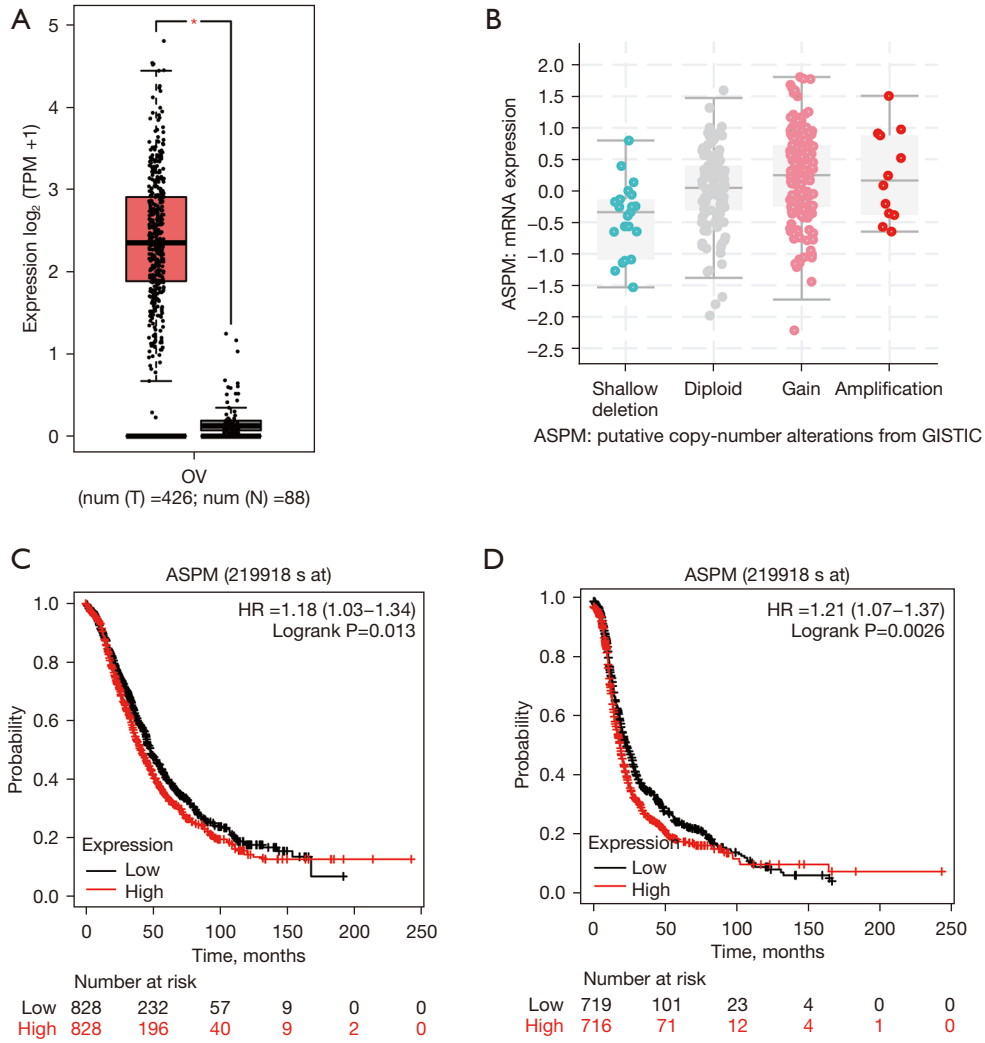

Figure 1 ASPM is highly expressed in OvCa and is related to poor prognosis of OvCa. (A) The expression of ASPM in the OvCa samples (n=426) was significantly higher than the normal samples (n=88). *P<0.05. (B) The copy number variable of ASPM in OvCa. (C) The relationship between the expression of ASPM and OS in patients with OvCa (n=1,657). (D) The relationship between the expression of ASPM and PFS in patients with OvCa (n=1,436). ASPM, spindle-like microcephaly-associated protein; OvCa, ovarian cancer; OS, overall survival; PFS, progression-free survival.

Statistical analysis

All statistical analyses were performed using SPSS version 22.0 (SPSS Inc., Chicago, IL, USA) and GraphPad Prism version 7.0 (GraphPadInc., San Diego, CA, USA). Comparisons between groups were analyzed using one-way ANOVA. χ^2 test or Fisher's exact test were used to analyze the correlation between IHC score and clinical characteristics. All cell experiments were independently replicated 3 times. A P value of <0.05 was considered statistically significant.

Results

ASPM overexpression predicts poor prognosis in OvCa patients

We used GEPIA 2.0 to perform differential expression analysis to compare ASPM expression in OvCa and normal ovary tissue from the TCGA database. Expression of ASPM was significantly higher in OvCa than normal ovary tissue (*Figure 1A*, log2FC cutoff >1, P<0.05). To further investigate ASPM gene alterations in OvCa,

© Gland Surgery. All rights reserved.

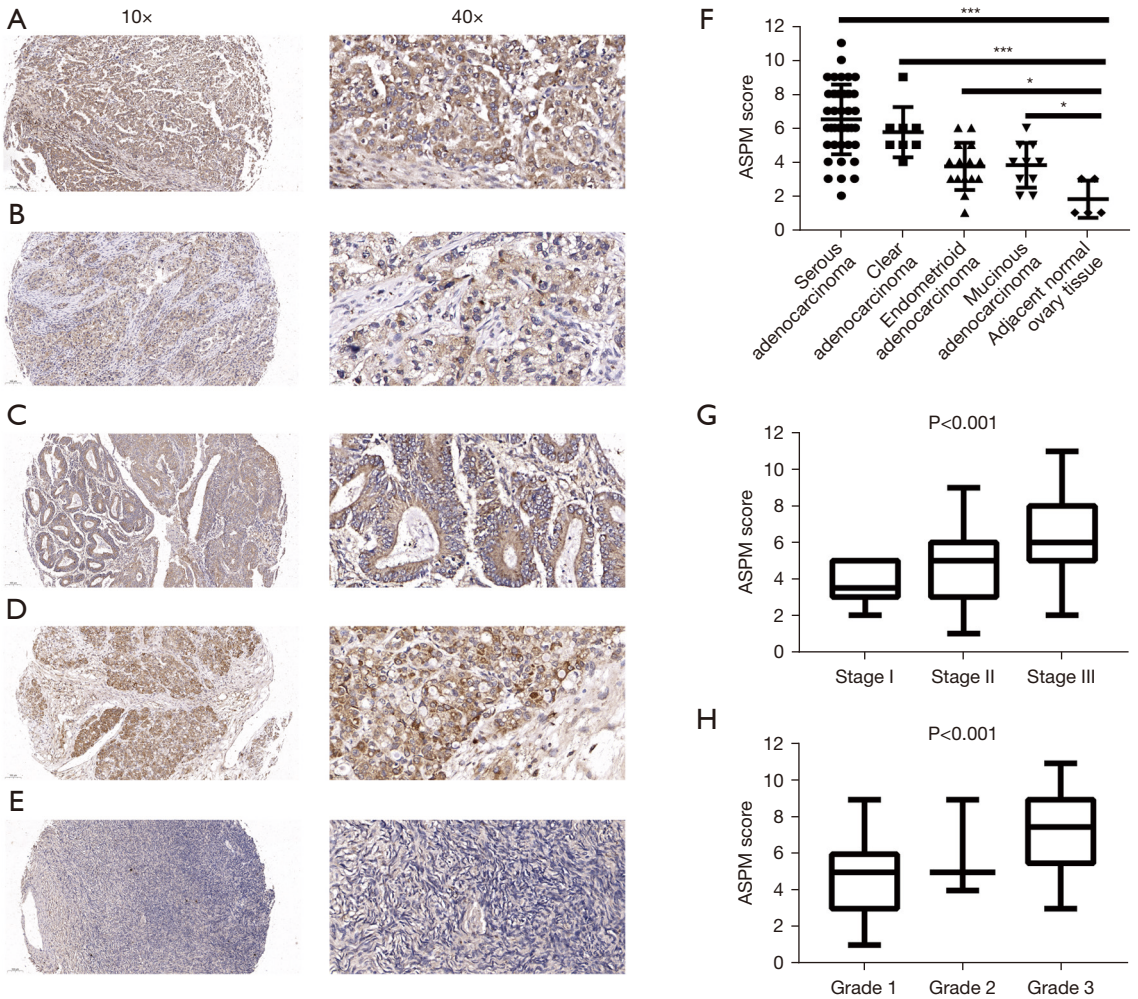

Figure 2 ASPM is highly expressed in EOC and is related to clinic stage and pathological grade of EOC. (A-E) Representative IHC photomicrographs of expression of ASPM in four subtype EOC tissues (serous adenocarcinoma, clear cell carcinoma, Endometrioid adenocarcinoma, Mucinous adenocarcinoma) and normal tissue stained by anti-rabbit-ASPM. (F) The IHC score of ASPM in four subtype EOC tissues and normal tissue. *P<0.05, ***P<0.001. (G) The IHC score of ASPM is related to clinical TNM stage of EOC. (H) The IHC score of ASPM is related to pathological grade of EOC. ASPM, spindle-like microcephaly-associated protein; EOC, epithelial ovarian cancer; IHC, immunohistochemistry; TNM, tumor-node-metastasis.

we used cBioPortal to analyze putative copy number alterations based on the TCGA dataset. We observed that ASPM gene alteration in OvCa was mainly gain and copy number amplification (*Figure 1B*). Further, we estimated the prognostic value of ASPM expression in patients with OvCa using Kaplan-Meier survival analysis. OvCa patients with higher ASPM expression had worse overall survival (OS) [*Figure 1C*, hazard ratio (HR) =1.18, P=0.013] and progress free survival (PFS) (*Figure 1D*, HR =1.21, P=0.0026). These results indicated that ASPM overexpression was closely associated with poor prognosis in OvCa patients, and that ASPM could have important oncogenic properties, suggesting it may be a reliable prognostic predictor in ovarian cancer.

ASPM overexpression in EOC is associated with clinical characteristics in TMA

To determine the clinical value of ASPM expression in the 4 EOC subtypes (*Figure 2A-2D*) and normal ovary samples (*Figure 2E*), we analyzed the IHC staining scores of an ovarian TMA, including 42 cases of serous adenocarcinoma,

© Gland Surgery. All rights reserved.

Table 1 Association of ASPM expression levels with different clinicopathologic characteristics in EOC

Clinicopathologic	ASPM expression, n (%)		P value
	Low count	High count	
Age, years			0.133
≤50	25 (65.8)	18 (48.6)	
>50	13 (34.2)	19 (51.4)	
Lymph node metastasis			0.030
N0	37 (97.4)	29 (78.4)	
N1	1 (2.6)	8 (21.6)	
TNM stage			0.008
Stage I	31 (81.5)	19 (51.4)	
Stage II	2 (5.3)	1 (2.7)	
Stage III	5 (13.2)	17 (45.9)	
Histologic grade			<0.0001
Grade 1	10 (26.3)	0 (0.0)	
Grade 2	16 (42.1)	11 (29.7)	
Grade 3	12 (31.6)	26 (70.3)	

P values were calculated by comparing the expression of ASPM with different clinical variables respectively using a chi-square test. P<0.05 was considered statistically significant. ASPM, spindle-like microcephaly-associated protein; TNM, tumor-node-metastasis; EOC, epithelial ovarian cancer.

Table 2 Association of ASPM expression levels with different clinicopathologic characteristics in serous adenocarcinoma

Clinicopathologic	ASPM expression, n (%)		P value
	Low count	High count	
Age, years			0.554
≤50	13 (59.1)	10 (50.0)	
>50	9 (40.9)	10 (50.0)	
Lymph node metastasis			0.043
N0	22 (100.0)	15 (75.0)	
N1	0 (0.0)	5 (25.0)	
TNM stage			0.002
Stage I	18 (81.9)	7 (35.0)	
Stage II	1 (4.5)	0 (0.0)	
Stage III	3 (13.6)	13 (65.0)	
Histologic grade			0.015
Grade 1	7 (31.8)	0 (0.0)	
Grade 2	4 (18.2)	3 (15.0)	
Grade 3	11 (50.0)	17 (85.0)	

P values were calculated by comparing the expression of ASPM with different clinical variables respectively using a chi-square test. P<0.05 was considered statistically significant. ASPM, spindle-like microcephaly-associated protein; TNM, tumor-node-metastasis.

8 clear cell carcinoma cases, 15 endometrioid adenocarcinoma cases, 10 mucinous adenocarcinoma cases, and 5 adjacent normal tissues. According to the immunostaining results, ASPM staining was localized to the nucleus and the cytoplasm, and ASPM was significantly overexpressed in the 4 EOC subtypes compared with normal ovary tissue (*Figure 2F*, P<0.05), which was consistent with the previous bioinformatics analysis.

Further, we explored the correlation between the IHC score of ASPM and clinical characteristics. We observed that samples with higher clinical stage and pathological grade had higher ASPM expression scores (*Figure 2G,2H*; P<0.001). We divided the patients into 2 groups (high expression subgroup and low expression subgroup) based on the mean IHC score. We then compared the differences in clinical characteristics between the 2 groups. Higher ASPM expression in patients with EOC predicted a more advanced clinical tumor-node-metastasis (TNM) stage, poorer histological grade, and positive lymph node metastasis. However, the correlation between ASPM score and patient age was not statistically significant (*Table 1*). In addition, we performed subgroup analysis with 42 serous adenocarcinoma cases and observed a similar result (*Table 2*). Our IHC analysis indicated that ASPM may have promoted ovarian cancer cell proliferation and migration.

ASPM is overexpressed in OVCAR3 and A2780 cells

In order to select cell lines with relatively high ASPM expression for subsequent cell function experiments, we compared ASPM expression in 3 common EOC cell lines, including OVCAR3, A2780, and ES-2. Among these cell lines, OVCAR3 and A2780 had higher ASPM mRNA and protein expression (*Figure 3A,3B*; P<0.05). We verified the effects of the 2 interference siRNAs by Western blotting and RT-qPCR in OVCAR3 and A2780 cells. Our results confirmed that the 2 siRNAs significantly reduced ASPM expression (*Figure 3C-3F*, P<0.05).

© Gland Surgery. All rights reserved.

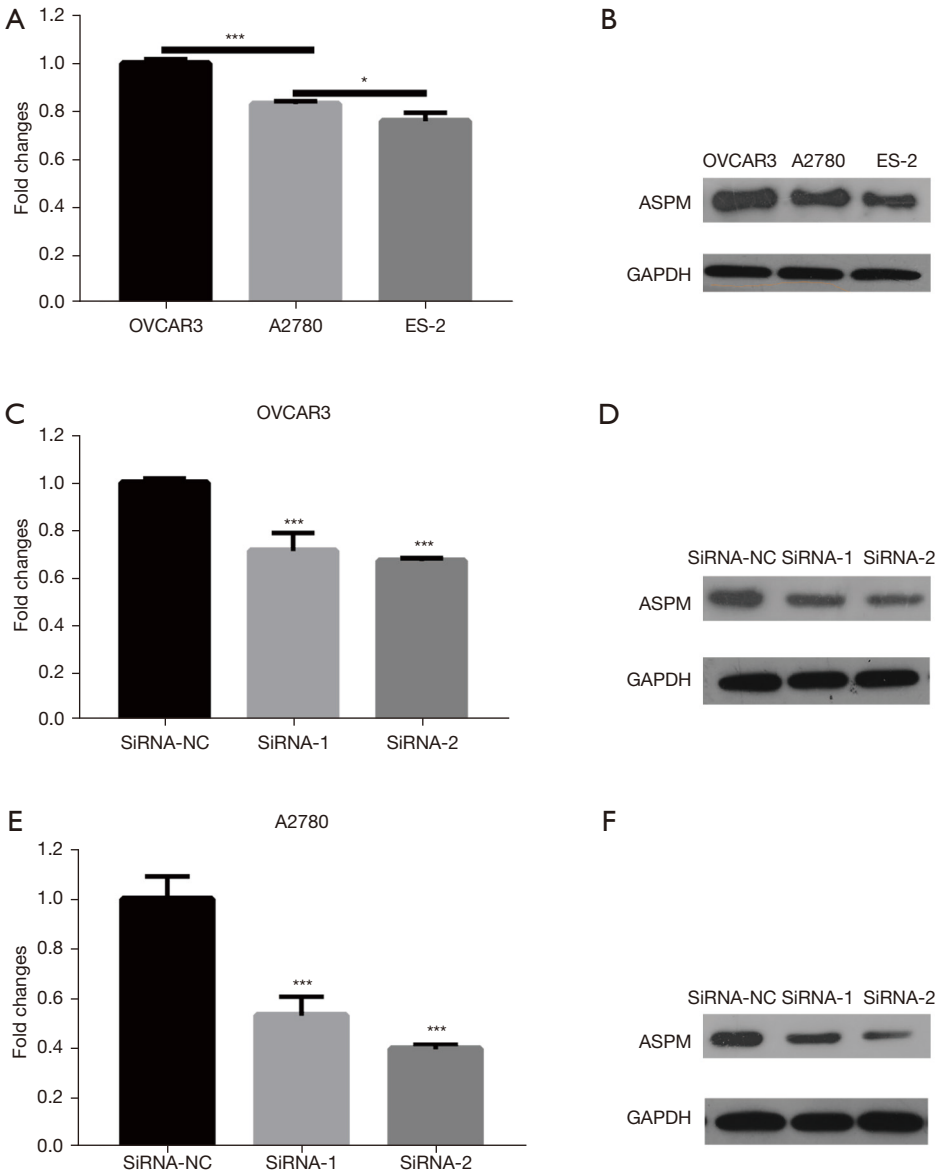

Figure 3 ASPM is highly expressed in OVCAR3 and A2780 cells. (A) Fold changes of ASPM mRNA in OVCAR3, A2780 and ES-2 cells. (B) Western blot analysis of ASPM expression in in OVCAR3, A2780 and ES-2 cells. (C) Fold changes of ASPM mRNA after knocking down in OVCAR3 cells. (D) Western blot analysis of ASPM expression after knocking down in OVCAR3 cells. (E) Fold changes of ASPM mRNA after knocking down in A2780 cells. (F) Western blot analysis of ASPM expression after knocking down in A2780 cells. Data are means ± SD of three independent experiments. *P<0.05, ***P<0.001. Total proteins (25 μg) were separated on SDS-PAGE and transferred to PVDF membranes. Proteins were detected using anti-ASPM and anti-GAPDH antibodies. ASPM, spindle-like microcephaly-associated protein; OVCAR3, human ovarian adenocarcinoma cell 3; SD, standard deviation; SDS-PAGE, dodecyl sulfate, sodium salt (SDS)-polyacrylamide gel electrophoresis; PVDF, polyvinylidene fluoride; GAPDH, glyceraldehyde-3-phosphate dehydrogenase.

ASPM promotes cell proliferation in vitro

Previous studies have indicated that ASPM may be involved in EOC progression (15,22,24,25); however, validation in knockdown cell models *in vitro* is still lacking. Therefore, we investigated whether ASPM influenced EOC progression in OVCAR3 and A2780 cells. We knocked down ASPM expression inOVCAR3 and A2780EOC cells using 2

© Gland Surgery. All rights reserved.

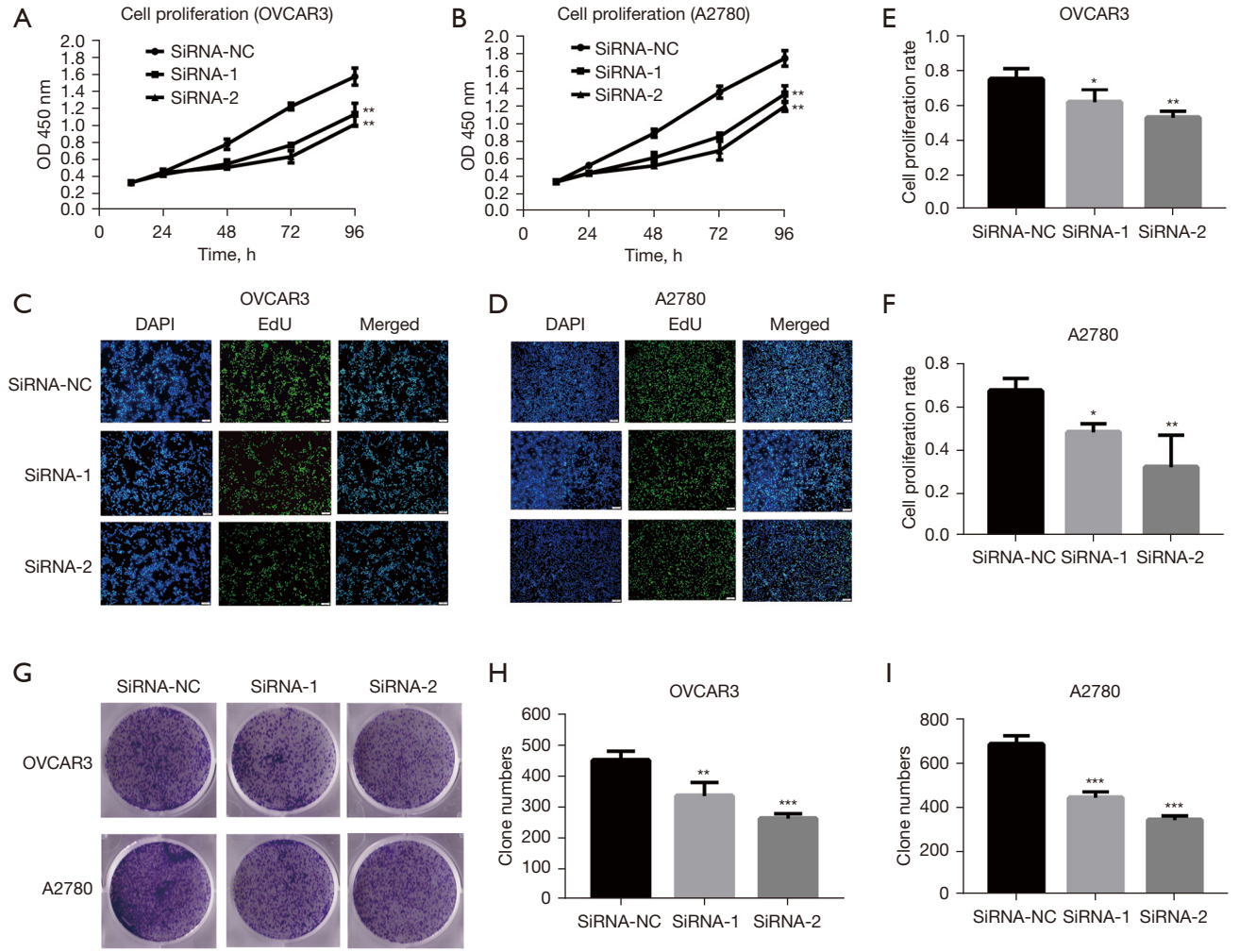

Figure 4 ASPM promoted cell proliferation in OVCAR3 and A2780 cells. (A,B) The proliferation capacity of OVCAR3 and A2780 cells was estimated by the CCK-8 assay. (C,D) The positive rate of cell proliferation of OVCAR3 and A2780 cells by EdU assay. The magnification is ×200. (E,F) Cell proliferation rate in OVCAR3 and A2780 cells was calculated by ImageJ. (G) Effect of ASPM on colony formation in OVCAR3 and A2780 cells stained by 2% crystal violet. The magnification is 0. (H-I) Quantitative changes in OVCAR3 and A2780 colony formation were evaluated by counting using ImageJ. Data represent the mean ± SD of three independent experiments. *P<0.05, **P<0.01, ***P<0.001. OVCAR3, human ovarian adenocarcinoma cell 3; SD, standard deviation; OD, optical density; CCK-8, cell counting kit-8.

targeted siRNAs. The 3 assays, including CCK-8, EdU, and colony-forming unit assays, were used to assess cell proliferation ability. ASPM knockdown significantly decreased OVCAR3 and A2780 cell proliferation compared to the negative control group via CCK-8 assay (*Figure 4A,4B*; P<0.05). Consistently, knocking down ASPM decreased the percentage of cells labeled with EdU in OVCAR3 and A2780 cells (*Figure 4C-4F*, P<0.05), suggesting ASPM silencing may have inhibited the DNA replication of cells. The colony-forming units in cells with ASPM-knockdown were significantly reduced compared to negative control siRNA (*Figure 4G-4I*, P<0.05).

ASPM promotes OVCAR3 and A2780 cell migration

The enhancement of cell migration is the biological basis of clinical OvCa progression and metastasis. Therefore, it was necessary to determine the influence of ASPM on EOC cell migration. We performed migration transwell assays using ASPM-knockdown OVCAR3 and A2780 cells and observed that ASPM silencing significantly inhibited the ability of cell migration (*Figure 5A,5B*; P<0.01).

© Gland Surgery. All rights reserved.

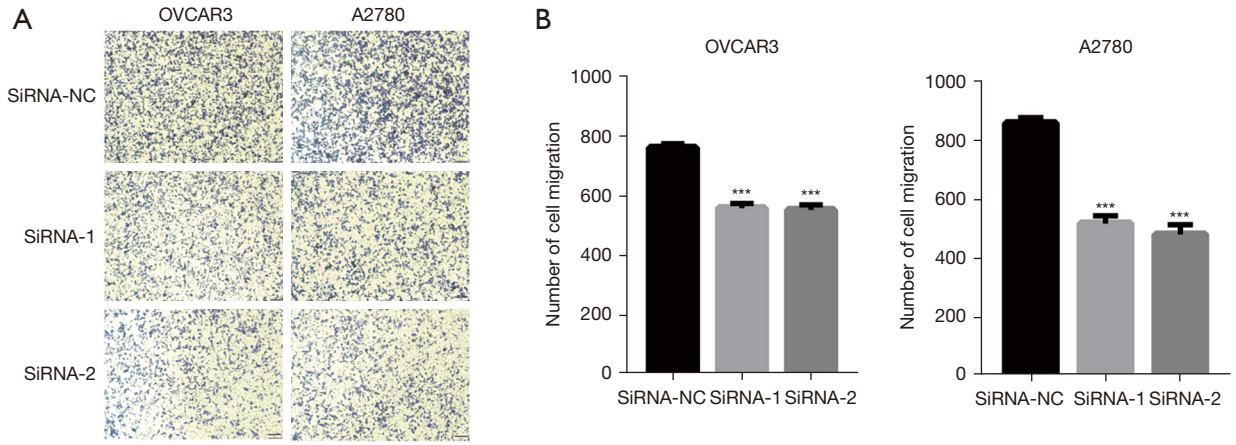

Figure 5 ASPM promoted cell migration in OVCAR3 and A2780 cells. (A) The cell migration stained by 2% crystal violet in OVCAR3 and A2780 cells determined by Transwell assay. The magnification is ×200. (B) Quantitative analysis of OVCAR3 and A2780 cells migration by ImageJ. Migration assays were performed in ASPM knockdown OVCAR3 and A2780 cells transfected with siRNAs and negative controls. Data represent the mean ± SD of three independent experiments. ***P<0.001. ASPM, spindle-like microcephaly-associated protein; OVCAR3, human ovarian adenocarcinoma cell 3; SD, standard deviation.

ASPM regulates the cell cycle inOVCAR3 and A2780 cells

To identify the potential downstream pathways of ASPM, differential expression analysis was carried out between the high- and low-ASPM subgroups divided by median expression level using the ovarian cancer expression matrix downloaded from TCGA. A total of 9,073differentially expressed genes (adjusted P<0.05) were selected out for subsequent analysis. To investigate the potential biological process regulated by ASPM in EOC cells in depth, we performed gene set enrichment analysis based on the above candidate genes via Web Gestalt analysis (KEGG pathway analysis). *Figure 6A* shows the top 20 functional pathways [false discovery rate (FDR) <0.05] that the candidate genes enriched. We found that the cell cycle signaling pathway was significantly enriched (*Figure 6B*) (FDR <0.05, P<0.001, normalized enrichment score =3.5371). *Figure 6C* shows the potential cell cycle-related genes which ASPM may have regulated.

In order to verify the above results, we performed flow cytometry to determine whether ASPM could regulate the cell cycle signaling pathway and the phase of the cell cycle it regulated in EOC. We transfected OVCAR3and A2780 cells with 2 siRNAs and analyzed the cell cycle distribution using flow cytometry (*Figure 7A*,*7B*). Flow cytometry analysis indicated that, compared to the siNC-transfected cells, the ASPM siRNA-transfected cells were arrested in the synthesis (S) phase (*Figure 7C*,*7D*). Our findings indicated that silencing ASPM could significantly inhibit EOC cell proliferation by inducing S phase arrest.

Discussion

Compared with other gynecological tumors, EOC involves early symptoms rarely detected, a high degree of malignancy, late clinical stage at diagnosis, and a relatively poor effect of clinical treatment (26). Therefore, the discovery of potential biomarkers is key to early diagnosis. ASPM participates in the occurrence, progression, and metastasis of various tumors (10,27). However, whether ASPM contributes to the proliferation of OvCa cells and its mechanism is unclear. In the present study, we used ASPM expression profiles from OvCa patients to confirm abnormally high ASPM expression in OvCa. Further, we observed that higher ASPM expression was related to worse prognosis in OvCa patients. TMA IHC analysis further confirmed that ASPM was overexpressed in OvCa tissues and correlated to clinical TNM stage, pathological grade, and lymphatic metastasis. Finally, we verified that ASPM promoted the proliferation and migration of EOC through cell experiments.

ASPM is one of the main pathogenic genes of autosomal recessive microcephaly disease, where it regulates the division and proliferation of neural stem cells (28). The protein encoded by ASPM is a spindle pole/intermediate protein that regulates the direction of mitosis and the

© Gland Surgery. All rights reserved.

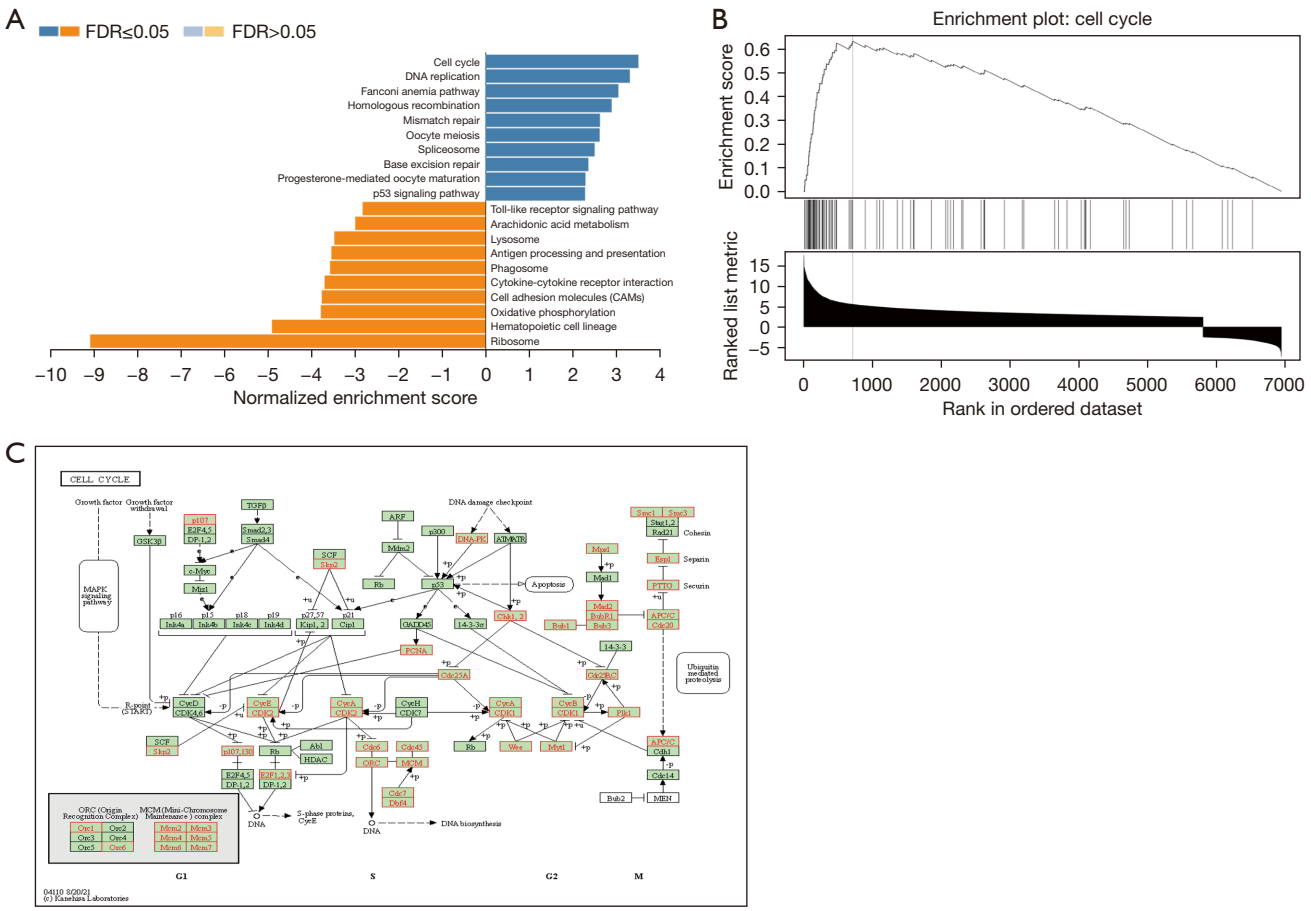

Figure 6 ASPM is associated with cell cycle pathway. (A) The top 20 functional pathways (FDR <0.05) which the DEGs enriched based on the web-based Gene Set Analysis Toolkit (http://www.webgestalt.org/). (B) GSEA of KEGG pathway gene sets in ASPM high versus low samples from TCGA database (FDR <0.05, P<0.001, Normalized Enrichment Score =3.5371). (C) The 39 potential cell cycle-related genes (red) which ASPM may regulated. ASPM, spindle-like microcephaly-associated protein; FDR, false discovery rate; GSEA, Gene Set Enrichment Analysis; KEGG, Kyoto Encyclopedia of Genes and Genomes.

division of cytoplasm. ASPM places a high value on the symmetrical division and proliferation of neuro-epithelial cells during brain development, and it shown that silencing ASPM significantly reduced symmetrical neuron division in the cerebral cortex of mice (5). ASPM protein change their location at different stages of cell division. During chromosome division, ASPM is located at the intermediate and spindle poles of the cell; during cytoplasmic division, ASPM accumulates at the intermediate loop. When ASPM is mutated, the function of the protein is affected, and consequently the function of the intermediate is defective leading to the failure of chromosome segregation, the emergence of heteroploidy and tumorigenesis. During tumorigenesis, both the symmetric/asymmetric cell division pattern and the orientation of the mitotic spindle are related to the site of cell division. In view of the function of ASPM on mitotic regulation, studies on the relevance of ASPM to tumorigenesis have been carried out. ASPM is overexpressed in diverse carcinomas and contributes to its progression. In brain gliomas, ASPM mRNA is significantly increased, and patients with higher ASPM mRNA expression have poorer prognosis. Several studies have confirmed that ASPM knock down expression significantly suppressed cell viability by inhibiting the Wnt-β-catenin pathway (8,29). One study reported that high ASPM expression in patients with endometrial carcinoma predicted poor prognosis (9). Similar results have been observed in bladder carcinoma (27), pancreatic adenocarcinoma (10), colonic

© Gland Surgery. All rights reserved.

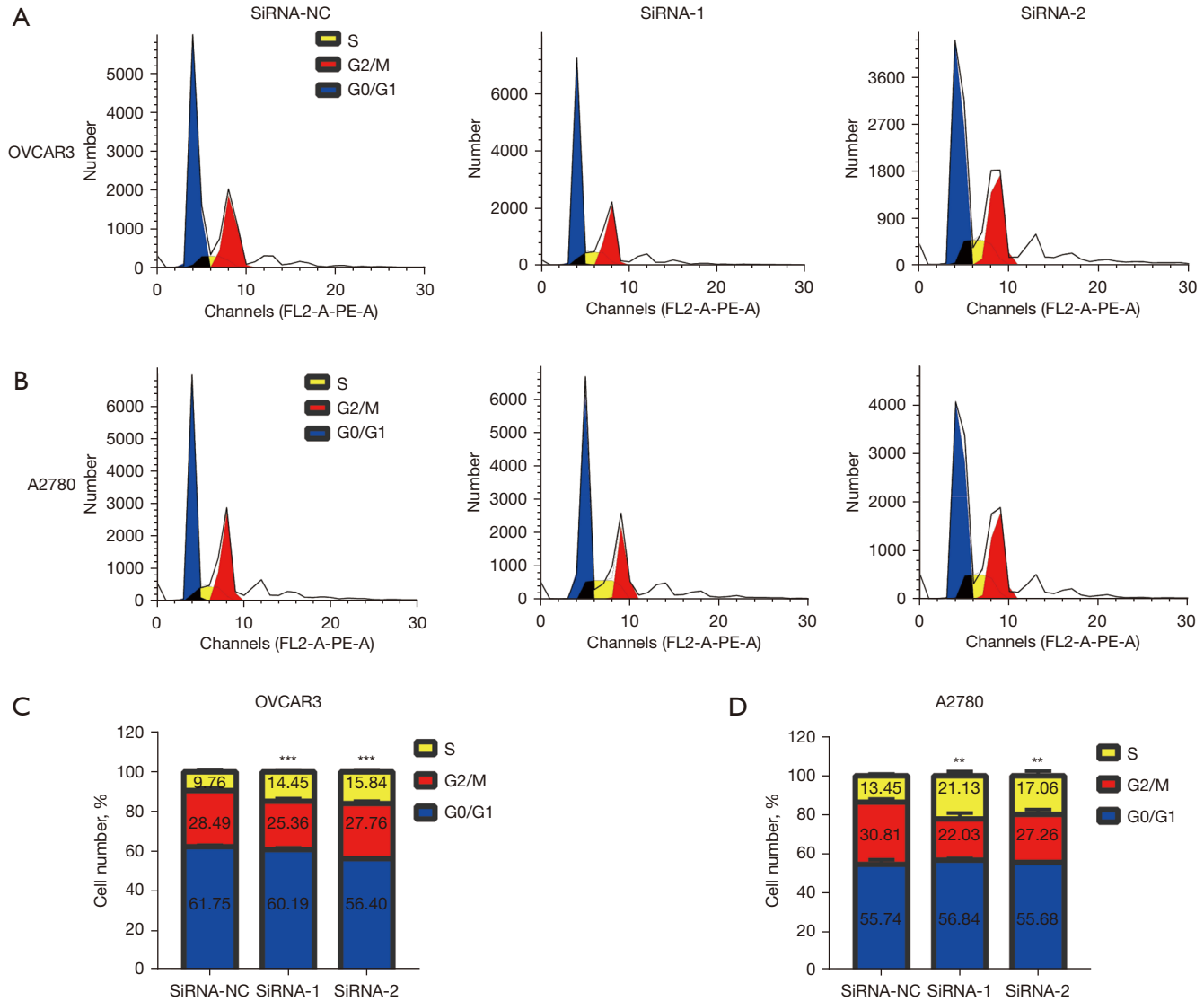

Figure 7 ASPM regulated the cell cycle of OVCAR3 and A2780 cells. (A) Cell cycle profile of ASPM-knockdown OVCAR3 cells determined by flow cytometry analysis. (B) Cell cycle profile of ASPM-knockdown A2780 cells determined by flow cytometry analysis. (C,D) The proportion of cells in each phase of the cell cycle was quantified concerning the total number of cells in OVCAR3 and A2780 cells. Results shown are representative of three independent experiments. **P<0.01, ***P<0.001. ASPM, spindle-like microcephaly-associated protein; OVCAR3, human ovarian adenocarcinoma cell 3.

adenocarcinoma (30), and prostate adenocarcinoma (11). A previous study, which cultured primary cells from the as cite of OvCa, found that the grade of OvCa was positively correlated with ASPM expression, and that patients with higher ASPM had relatively shorter survival time (14). Further IHC analysis showed that with increased tumor grade, the expression of ASPM gradually increased, and cases with high expression of ASPM were more likely to have lymph metastasis (15). Our data mining analysis and IHC results were consistent with previous conclusions. We also confirmed that ASPM was related to clinical stage, pathological grade, and lymph node metastasis. *Figure 1B* showed the pattern of ASPM copy number alteration in OvCa was mainly gain and copy number amplification. Therefore, based on the previous findings, subsequently, we confirmed that ASPM promoted the proliferation and migration of OvCa cells by knocking down ASPM *in vitro*.

In order to explore the downstream pathways that ASPM

© Gland Surgery. All rights reserved.

may regulate in EOC, we conducted KEGG pathway enrichment analysis, which confirmed that ASPM may have regulated cell cycle signaling pathways. Further, flow cytometry confirmed that ASPM downregulation caused cell cycle arrest in the S phase. The cell cycle is the main stage in the process of cell proliferation, and a common mechanism in tumorigenesis is disorder of the cell cycle. Consistent with the results of our analysis, ASPM is closely related to the spindle function which regulates the direction of mitosis and cytoplasmic division during the cell cycle and participates in the progress of the cell cycle, thereby affecting the growth of cells. A study has shown that ASPM is a positive regulator of Wnt pathway which is a key regulator of cell cycle. Knockout of ASPM gene reduces the protein expression of β-catenin, DVL2 and DVL3 and arrest the cycle in the gap 1 (G1) phase (8). It can be seen that ASPM can indirectly affect the stability of β-catenin by directly regulating the stability of DVL3 and DVL2 protein, thereby regulating the Wnt signaling pathway. Further, ASPM has been found to interact with the cyclin-dependent kinase 2 (Cdk2)/Cyclin E complex, regulating cyclin activity by modulating its ubiquitination, phosphorylation, and localization into the nucleus before the cell is fated to transverse the restriction point (31). In addition, the transcription factor FOXM1 directly bound to the ASPM promoter and activated the transcription of ASPM, regulating the Wnt signaling pathway (29). In breast cancer, however, after silencing ASPM, the formation of microtubule structures in the nucleus of cells is blocked, causing cell cycle arrest in the G2/mitosis (M) stages of the cell cycle and leading to apoptosis (32). The differences in ASPM regulation of the tumor cell cycle may depend on the different potential functions of ASPM in various tumors or tumor heterogeneity.

Our research had some limitations. First, because the TMA we purchased lacked prognostic data, the relationship between ASPM expression and prognosis of clinical OvCa patient was unclear. Second, while we verified that ASPM promoted the proliferation of OvCa cells using *in vitro* cell experiments, xenograft mouse models are needed in future research. Third, we performed KEGG pathway analysis and flow cytometry to determine that ASPM knockdown could block S phase of EOC cell cycle, but the specific molecular pathway involved in cell cycle regulation by ASPM remains to be elucidated.

Conclusions

In conclusion, our study confirmed that ASPM promoted proliferation by regulating the cell cycle in epithelial ovarian cancer, suggesting that ASPM may be a novel biomarker for early screening in EOC and may be a therapeutic target in the future.

Acknowledgments

Funding: The study was supported by the National Natural Science Foundation of China (No. 81760504 and No. 82160454), the Youth Fund Project of Jiangxi Provincial Department of Education (No. GJJ200252), the Graduate Innovation Foundation of Jiangxi Province (No. YC2020-B045), the Science and Technology Project of Health Commission of Jiangxi Province, China (No. 202130409), and the Science and Technology Project of Jiangxi Provincial Administration of Traditional Chinese Medicine, China (No. 2020A0051).

Footnote

Reporting Checklist: The authors have completed the MDAR reporting checklist. Available at https://gs.amegroups.com/article/view/10.21037/gs-22-29/rc

Data Sharing Statement: Available at https://gs.amegroups.com/article/view/10.21037/gs-22-29/dss

Conflicts of Interest: All authors have completed the ICMJE uniform disclosure form (available at https://gs.amegroups.com/article/view/10.21037/gs-22-29/coif). The authors have no conflicts of interest to declare.

Ethical Statement: The authors are accountable for all aspects of the work in ensuring that questions related to the accuracy or integrity of any part of the work are appropriately investigated and resolved. All experiments were approved by the Ethics Committee of the Second Affiliated Hospital of Nanchang University [REVIEW(2020) No.(010)] and patient consent was acquired. The study was conducted in accordance with the Declaration of Helsinki (as revised in 2013).

Open Access Statement: This is an Open Access article distributed in accordance with the Creative Commons Attribution-NonCommercial-NoDerivs 4.0 International License (CC BY-NC-ND 4.0), which permits the non-commercial replication and distribution of the article with the strict proviso that no changes or edits are made and the

© Gland Surgery. All rights reserved.

original work is properly cited (including links to both the formal publication through the relevant DOI and the license). See: https://creativecommons.org/licenses/by-nc-nd/4.0/.

References

1. Siegel RL, Miller KD, Fuchs HE, et al. Cancer Statistics, 2021. CA Cancer J Clin 2021;71:7-33.
2. Köbel M, Kalloger SE, Boyd N, et al. Ovarian carcinoma subtypes are different diseases: implications for biomarker studies. PLoS Med 2008;5:e232.
3. Zhou W, Sun W, Yung MMH, et al. Autocrine activation of JAK2 by IL-11 promotes platinum drug resistance. Oncogene 2018;37:3981-97.
4. Liu Y, Li W, Luo J, et al. Cysteine-Rich Intestinal Protein 1 Served as an Epithelial Ovarian Cancer Marker via Promoting Wnt/β-Catenin-Mediated EMT and Tumour Metastasis. Dis Markers 2021;2021:3566749.
5. Garrett L, Chang YJ, Niedermeier KM, et al. A truncating Aspm allele leads to a complex cognitive phenotype and region-specific reductions in parvalbuminergic neurons. Transl Psychiatry 2020;10:66.
6. Kouprina N, Pavlicek A, Collins NK, et al. The microcephaly ASPM gene is expressed in proliferating tissues and encodes for a mitotic spindle protein. Hum Mol Genet 2005;14:2155-65.
7. Autosomal recessive primary microcephaly due to ASPM mutations: An update. Hum Mutat 2019;40:127. Erratum for: Hum Mutat 2018;39:319-332.
8. Chen X, Huang L, Yang Y, et al. ASPM promotes glioblastoma growth by regulating G1 restriction point progression and Wnt-β-catenin signaling. Aging (Albany NY) 2020;12:224-41.
9. Zhou JW, Wang H, Sun W, et al. ASPM is a predictor of overall survival and has therapeutic potential in endometrial cancer. Am J Transl Res 2020;12:1942-53.
10. Hsu CC, Liao WY, Chan TS, et al. The differential distributions of ASPM isoforms and their roles in Wnt signaling, cell cycle progression, and pancreatic cancer prognosis. J Pathol 2019;249:498-508.
11. Pai VC, Hsu CC, Chan TS, et al. ASPM promotes prostate cancer stemness and progression by augmenting Wnt-Dvl-3-β-catenin signaling. Oncogene 2019;38:1340-53.
12. Hao W, Zhao H, Li Z, et al. Identification of potential markers for differentiating epithelial ovarian cancer from ovarian low malignant potential tumors through integrated bioinformatics analysis. J Ovarian Res 2021;14:46.
13. Ye Q, Lei L, Aili AX. Identification of potential targets for ovarian cancer treatment by systematic bioinformatics analysis. Eur J Gynaecol Oncol 2015;36:283-9.
14. Brüning-Richardson A, Bond J, Alsiary R, et al. ASPM and microcephalin expression in epithelial ovarian cancer correlates with tumour grade and survival. Br J Cancer 2011;104:1602-10.
15. Alsiary R, Brüning-Richardson A, Bond J, et al. Deregulation of microcephalin and ASPM expression are correlated with epithelial ovarian cancer progression. PLoS One 2014;9:e97059.
16. Tang Z, Li C, Kang B, et al. GEPIA: a web server for cancer and normal gene expression profiling and interactive analyses. Nucleic Acids Res 2017;45:W98-W102.
17. Gao J, Aksoy BA, Dogrusoz U, et al. Integrative analysis of complex cancer genomics and clinical profiles using the cBioPortal. Sci Signal 2013;6:pl1.
18. Tang Z, Kang B, Li C, et al. GEPIA2: an enhanced web server for large-scale expression profiling and interactive analysis. Nucleic Acids Res 2019;47:W556-60.
19. Wu P, Heins ZJ, Muller JT, et al. Integration and Analysis of CPTAC Proteomics Data in the Context of Cancer Genomics in the cBioPortal. Mol Cell Proteomics 2019;18:1893-8.
20. Jiao XD, Qin BD, You P, et al. The prognostic value of TP53 and its correlation with EGFR mutation in advanced non-small cell lung cancer, an analysis based on cBioPortal data base. Lung Cancer 2018;123:70-5.
21. Nagy Á, Lánczky A, Menyhárt O, et al. Validation of miRNA prognostic power in hepatocellular carcinoma using expression data of independent datasets. Sci Rep 2018;8:9227.
22. Sun CC, Li SJ, Hu W, et al. Comprehensive Analysis of the Expression and Prognosis for E2Fs in Human Breast Cancer. Mol Ther 2019;27:1153-65.
23. Hou GX, Liu P, Yang J, et al. Mining expression and prognosis of topoisomerase isoforms in non-small-cell lung cancer by using Oncomine and Kaplan-Meier plotter. PLoS One 2017;12:e0174515.
24. Ning G, Huang YL, Zhen LM, et al. Transcriptional expressions of Chromobox 1/2/3/6/8 as independent indicators for survivals in hepatocellular carcinoma patients. Aging (Albany NY) 2018;10:3450-73.
25. Hu G, Yan Z, Zhang C, et al. FOXM1 promotes hepatocellular carcinoma progression by regulating KIF4A expression. J Exp Clin Cancer Res 2019;38:188.
26. Saeaib N, Peeyananjarassri K, Liabsuetrakul T, et al. Hormone replacement therapy after surgery for

© Gland Surgery. All rights reserved.

epithelial ovarian cancer. Cochrane Database Syst Rev 2020;1:CD012559.
27. Xu Z, Zhang Q, Luh F, et al. Overexpression of the ASPM gene is associated with aggressiveness and poor outcome in bladder cancer. Oncol Lett 2019;17:1865-76.
28. Johnson MB, Sun X, Kodani A, et al. Aspm knockout ferret reveals an evolutionary mechanism governing cerebral cortical size. Nature 2018;556:370-5.
29. Zeng WJ, Cheng Q, Wen ZP, et al. Aberrant ASPM expression mediated by transcriptional regulation of FoxM1 promotes the progression of gliomas. J Cell Mol Med 2020;24:9613-26.
30. An X, Huang Y, Zhao P. Expression of ASPM in colonic adenocarcinoma and its clinicopathologic significance. Int J Clin Exp Pathol 2017;10:8968-73.
31. Capecchi MR, Pozner A. ASPM regulates symmetric stem cell division by tuning Cyclin E ubiquitination. Nat Commun 2015;6:8763.
32. Komatsu M, Yoshimaru T, Matsuo T, et al. Molecular features of triple negative breast cancer cells by genome-wide gene expression profiling analysis. Int J Oncol 2013;42:478-506.

(English Language Editor: A. Muijlwijk)

Cite this article as: Wu Y, You Y, Chen L, Liu Y, Liu Y, Lou W, Fu F. Abnormal spindle-like microcephaly-associated protein promotes proliferation by regulating cell cycle in epithelial ovarian cancer. Gland Surg 2022;11(4):687-701. doi: 10.21037/gs-22-29

© Gland Surgery. All rights reserved.